Electronic Supplementary Material (ESI) for Lab on a Chip
This journal is © The Royal Society of Chemistry 2013

Supplementary Information for Continuous fractionation of cells and synthetic particles using an array of slanted cavities

Jorge A. Bernate,[1] Liu Chengxun,[2] Konstantinos Konstantopoulos,[1] Liesbet Lagae,[3] and German Drazer[1]

[1]*Department of Chemical and Biomolecular Engineering, Johns Hopkins University, Baltimore MD, 21218*

[2]*Interuniversity Microelectronics Center (IMEC), Kapeldreef 75, Heverlee 3001*

[3]*Interuniversity Microelectronics Center (IMEC), Kapeldreef 75, Heverlee 3001, and Katholieke Universiteit Leuven, Leuven 3000, Belgium*

Electronic Supplementary Material (ESI) for Lab on a Chip
This journal is © The Royal Society of Chemistry 2013

I. COMPUTATION OF THE PARTICLE-FREE FLOW

We numerically computed the Stokes flow field in an unbounded system using COMSOL Multiphysics® (COMSOL). The computational domain corresponds to a unit cell representing of the periodic system. The channel is 300 μm tall. The ridges are 25 or 10 μm tall, and the width and a spacing are 100 or 50 μm, respectively. The cross section of the unit cell comprises a cavity and half of a ridge on either side of the cavity. To reduce computational cost, the unit cell was 2 μm in the invariant direction (along the cavities), comprising only two layers of nodes in the numerical calculations. These cross-sections were meshed *extra fine* with physics controlled meshing to resolve the orientation angle of the flow in the recirculating regions in the corner of the cavities. The no slip condition was imposed on the bottom and upper walls while periodic boundary conditions were imposed on the side boundaries. The components of pressure drop per unit length imposed along and across the cavities were equal. This results in a direction of the flow in the vicinity of the upper wall $\alpha \approx 45^\circ$, which corresponds to the experimental conditions.

II. MEASUREMENT OF THE DEFLECTION ANGLE

The deflection angle for any given type of particle or cell was calculated as the difference between the approach angle on the plain region and the migration angle in the patterned region. The approach angle was calculated by tracking particles over a distance of about 100 μm on the plain region, with the final point of the trajectories being 100 μm away from the patterned region. The migration angle was calculated by measuring particle displacements between two points across a unit cell, in the middle of the cross-section of the device and about 1 mm into the patterned region. The values and error bars reported in Figs. 3, 6, and 7 are averages and standard deviations of at least 20 angle measurements of different particles/cells.

This journal is © The Royal Society of Chemistry 2013

III. CAPTION TO ESI MOVIES

ESI Movie 1

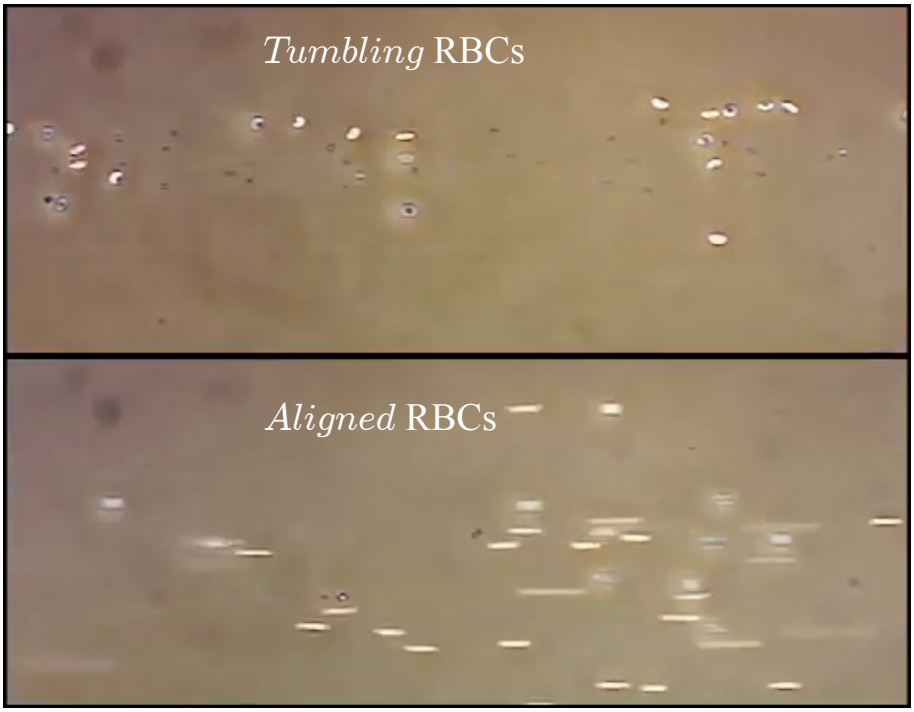

MOVIE 1. Phase contrast microscopy video showing the modes of motion of red blood cells (RBCs) at low (top) and high (bottom) velocities. At low velocities, RBCs *tumble* and appear to *blink* as they are carried by the flow. At high velocity, RBCs align one of their axis with the flow and appear as bright ellipsoids.

This journal is © The Royal Society of Chemistry 2013

ESI Movie 2

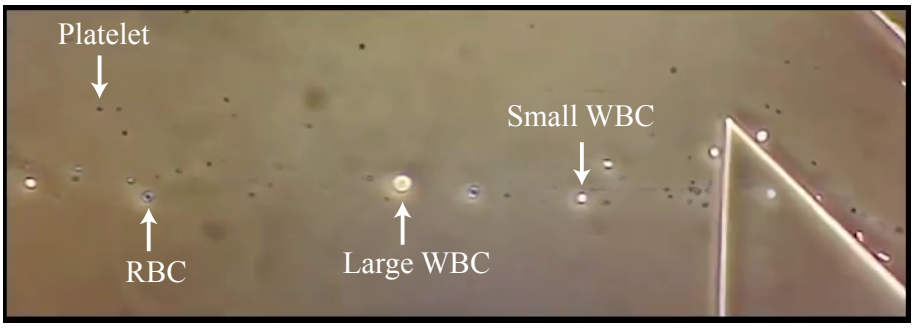

MOVIE 2. Phase contrast microscopy video showing red blood cells (RBCs), white blood cells (WBCs), and platelets. RBCs appear dark in the center and bright in the surrounding area and show different modes of motion (see ESI Movie 1). WBCs appear round and bright and do not deform considerably as they flow. Subpopulations of *small* and *large* WBCs could be distinguished. Platelets appear as dark spots, much smaller than RBCs and WBCs.

This journal is © The Royal Society of Chemistry 2013

ESI Movie 3

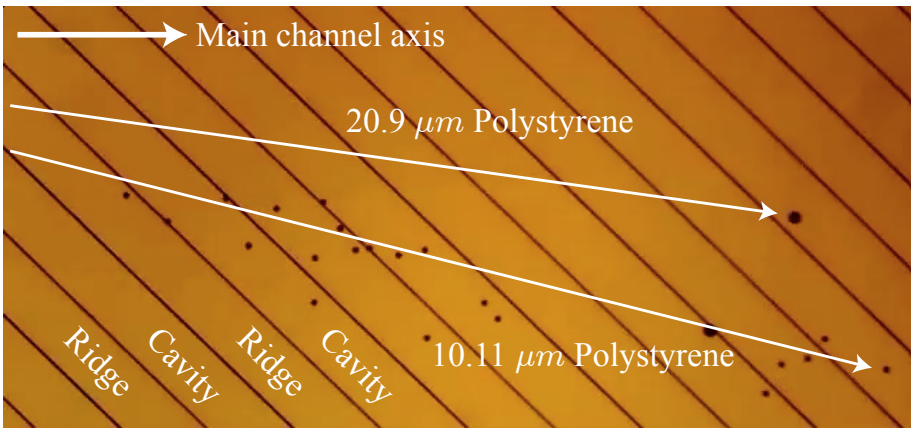

MOVIE 3. Deflection of the 10.11 and 20.9 μm polystyrene particles (buoyant density $\Delta\rho = 0.06$ g/mL). The ridges are 25 μm tall, 100 μm wide and separated by 100 μm. The particles travel in the direction of the imposed flow over the ridges and are deflected laterally as they traverse the cavities, with the smaller particles deflecting to a larger extent than the larger ones. This behavior, along with the characteristics of the particle-free flow (Fig. 5 in the main manuscript), indicate that the deflection of the particles is due to flow along the cavities; smaller particles are advected by the flow deeper into the cavities than the bigger particles and thus deflect more.

This journal is © The Royal Society of Chemistry 2013

ESI Movie 4

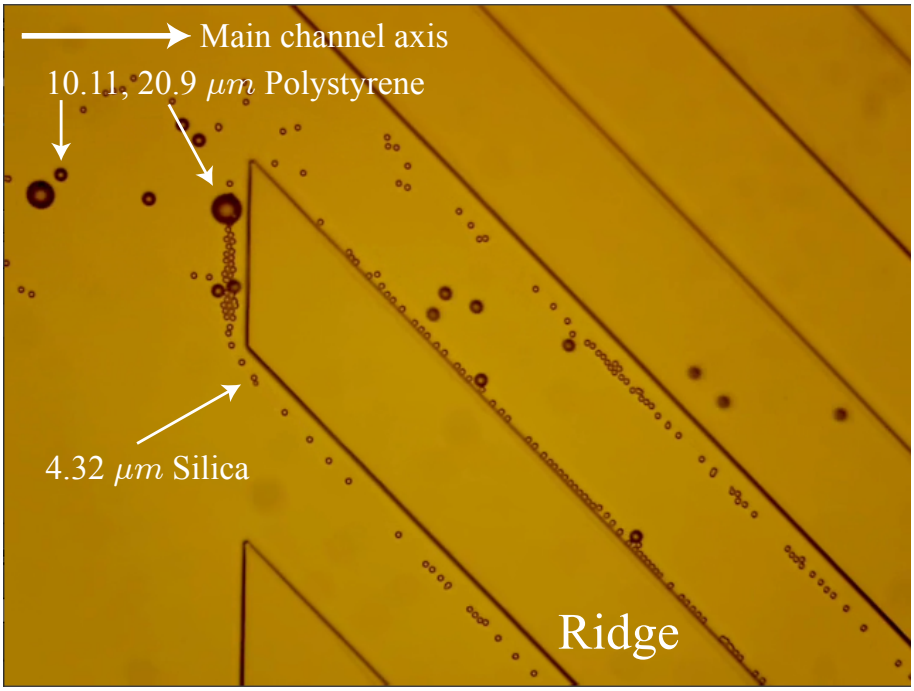

MOVIE 4. Behavior of 4.32 μm silica particles (buoyant density $\Delta\rho = 0.96$ g/mL) and of 10.11 and 20.9 μm polystyrene particles (buoyant density $\Delta\rho = 0.06$ g/mL) as they enter the patterned area. The ridges are 25 μm tall, 100 μm wide and separated by 100 μm. The 4.32 μm silica particles migrate towards the walls of the ridges after entering into the cavities; those moving in the vicinity of the reentrant or downstream corner attain an equilibrium distance from the wall of several microns, while those moving along the entrant corner do so in close proximity to the wall. Most of the polystyrene particles are carried over the ridges; a few of the 10.11 μm ones are confined to move along the entrant corner. These observations are consistent with the existence and characteristic size of the corotating recirculation regions at the corner of the cavities present in the particle free-flow.

This journal is © The Royal Society of Chemistry 2013

ESI Movie 5

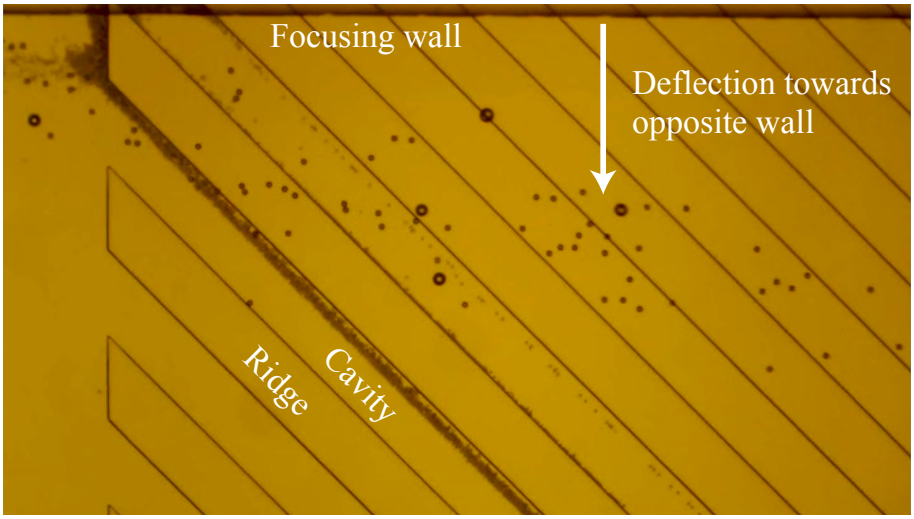

MOVIE 5. Separation and collection of silica microspheres (buoyant density $\Delta\rho = 0.96$ g/mL) with particle diameter of 4.32 μm, and polystyrene microspheres (buoyant density $\Delta\rho = 0.06$ g/mL) with diameters of 10.11 and 20.9 μm. The ridges are 25 μm tall, 100 μm wide, and separated by 100 μm. The particles are allowed to sediment to bottom surface of the device and then flow focused to the vicinity of one of the walls of the main channel (upper wall in the picture) before reaching the area patterned with the open cavities, where they deflect away from the focusing wall towards the opposite wall. The 4.32 μm silica particles remain confined to flow along the cavities and exit the patterned area in the bottom (outlet channel 1) with very high purity ($> 99\%$). The small contamination is due to a few 10.11 μm polystyrene particles that are trapped in the recirculating regions at the bottom corners of the cavity (see Movie 4). The outlet channels at the end of the patterned area are numbered starting from the channel opposite to the focusing wall (bottom wall in the movie). No particles exit in channel 2. The 10.11 μm polystyrene particles exit in channel 3 with 100% purity, and in channel 4 with a few contaminating 20.9 μm polystyrene particles (98% purity of 10.11 μm particles). The 20.9 μm particles exit with very high purity in channel 5 (94%), with a few contaminating 10.11 μm polystyrene particles. The collection data is given in Table I.

This journal is © The Royal Society of Chemistry 2013

	20.9 μm PS		10.11 μm PS		4.32 μm SiO_2		
Outlet channel	count	Purity %	count	Purity %	count	Purity %	t (sec)
5	17	94.44	1	5.56	0	0	47
4	2	1.92	51	98.08	0	0	47
3	0	0	> 100	100	0	0	25
2	0	NA	0	NA	0	NA	25
1	0	0	1	< 1	> 100	> 99	20

TABLE I. Particle collection data corresponding to Movie 5. The channels were in the field of view for the time indicated in the last column.

This journal is © The Royal Society of Chemistry 2013

ESI Movie 6

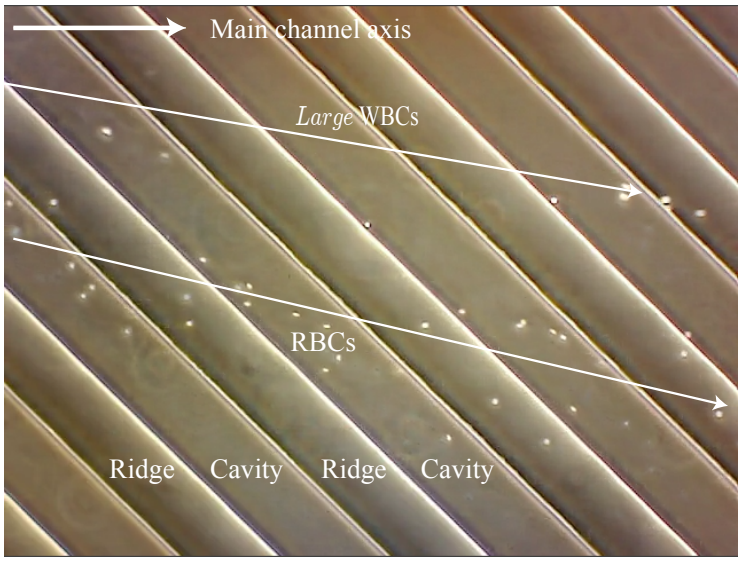

MOVIE 6. Phase contrast microscopy video showing the separation of *large* white blood cells and red blood cells in the device with ridges that are 25 μm tall, 100 μm wide and separated by 100 μm.